Remote Sensing of Environment 263 (2021) 112568

Contents lists available at ScienceDirect

Remote Sensing of Environment

journal homepage: www.elsevier.com/locate/rse

Phenology-based classification of invasive annual grasses to the species level

Peter J. Weisberg [a,*], Thomas E. Dilts [a], Jonathan A. Greenberg [a], Kerri N. Johnson [b,1], Henry Pai [b,2], Chris Sladek [b], Christopher Kratt [b], Scott W. Tyler [b], Alice Ready [a]

[a] Department of Natural Resources and Environmental Science, University of Nevada, Reno, 1664 N. Virginia Street, Mail Stop 0186, Reno, NV 89557, USA
[b] Department of Geologic Sciences and Engineering, University of Nevada, Reno, 1664 N. Virginia Street, Mail Stop 0172, Reno, NV 89557, USA

ARTICLE INFO

Editor: Marie Weiss

Keywords:
Medusahead
Taeniatherum caput-medusae
Cheatgrass
Bromus tectorum
Weed detection
Invasive plants
UAS
Multi-temporal classification
Plant phenology

ABSTRACT

The ability to detect and map invasive plants to the species level, both at high resolution and over large extents, is essential for their targeted management. Yet development of such remote sensing methodology is challenged by the spectral and structural similarities among many invasive and native plant species. We developed a multi-temporal classification approach that uses unoccupied aerial vehicles (UAV) imagery to map two invasive annual grasses to the species level, and to distinguish these from key functional types of native vegetation, based upon differences in plant phenology. For a case study area in the western Great Basin, USA, we intentionally over-sampled with frequent ($n = 8$) UAV flights over the growing season. Using this information we compared the importance of spectral variation at a given point in time (i.e., with and without near-infrared wavelengths), with spectral variation across multiple time periods. We found that differences in species phenology allowed for accurate classification of nine cover types, including the two annual grass species of interest, using just three dates of imagery that captured species-specific differences in the timing of active growth, seed head production, and senescence. Availability of near-infrared imagery proved less important than true-color RGB imagery collected at appropriate time periods. Thus, multi-temporal information provides a substitute for more extensive spectral information obtained from a single point in time. The substitution of temporal for spectral information is particularly well suited to UAV remote sensing, where the timing of image collection can be flexible. The datasets arising from our multi-temporal classification approach provide high-resolution information for modeling patterns of invasive plant spread, for quantifying plant invasion risk, and for early detection of novel plant invasions when patch sizes are still small. Widespread application and up-scaling of our approach requires advances in our ability to model the variability in phenology that occurs across years and over fine spatial scales, even within a single species.

1. Introduction

Invasive plant species rank as one of the greatest threats to biodiversity worldwide (Pimentel et al., 2001; Wilcove et al., 1998), and their control is critical for maintaining both economic and ecological values in socio-ecosystems already threatened by global environmental change. Control of invasive plants requires the application of management treatments that are carefully calibrated towards species-specific phenology and life history traits. For example, the application of post-emergent herbicides to reduce the establishment of invasive annual grasses is most effective when targeted to the period of emergence for a given species (Marushia et al., 2010). Also, treatments that reduce the population size of one invasive plant species may lead to population increases in a different, competing invasive plant species (e.g. Ogden and Rejmánek, 2005), requiring careful monitoring of treatment outcomes. Thus, the targeted control of invasive plants depends upon development of efficient and scalable methodologies for mapping them to the species level.

Successful approaches to classification of invasive plants have commonly capitalized on species-specific differences in phenology

* Corresponding author.
E-mail address: pweisberg@unr.edu (P.J. Weisberg).
[1] Present address: Department of Integrative Biology, University of California, Berkeley.
[2] Present address: Northwest River Forecast Center, National Oceanic and Atmospheric Administration, Portland, Oregon.

https://doi.org/10.1016/j.rse.2021.112568
Received 30 January 2021; Received in revised form 14 June 2021; Accepted 16 June 2021
Available online 21 June 2021

(Bradley and Mustard, 2006; Peterson, 2005), given that many plant species are spectrally and structurally quite similar but may exhibit important differences in the timing of key events in their life cycle, such as green-up, maximum growth, flowering, fruit and seed production, and vegetative senescence. Indeed, it is often possible to distinguish invasive species from co-occurring vegetation using a single image acquisition that is carefully timed to a particular phenological event such as flowering stage (e.g. *Lepidium latifolium* in California, USA, Andrew and Ustin, 2009; *Jacobaea vulgaris* in Schleswig-Holstein, Germany, Tay et al., 2018). However, high resolution, phenological mapping of invasive weeds focusing on flowering cycles poses practical implementation challenges. While high-resolution (< 1 m pixel size), hyperspectral imagery is becoming more available and affordable, primarily using UAVs, large-scale hyperspectral sensors with high spatial resolution do not currently exist, so the ability to scale these approaches is limited. Furthermore, due to the logistical constraints of flight and image acquisition planning, leveraging flowering phenology presupposes the analyst knows when the flowering events will occur ahead of time (Müllerová et al., 2017); however, the flowering timing likely changes from year-to-year and across a landscape. Thus, leveraging phenology in a practical sense would benefit from a fixed set of start and stop times during a growing season, with multiple acquisitions within this time window that, in theory, cover the variability in both vegetative and reproductive phenology for each species without needing to time collections to a specific phenological event. Such an approach requires a multi-temporal classification method that incorporates spectral information from throughout the growing season, and possibly the dormant season as well. For example, Martin et al. (2018) had success mapping invasive Asian knotweed species (*Fallopia japonica*; *Fallopia* x *bohemica*) using UAV imagery and a multi-temporal classification approach incorporating spectral indices from multiple image collection dates.

Multi-temporal classification approaches have been applied to mapping of invasive annual grass species in the western United States, emphasizing the prevalent invader cheatgrass (*Bromus tectorum*) and most commonly relying on inter- or intra-annual spectral differences between the active growing season and the senescent period (Boyte et al., 2016; Bradley and Mustard, 2006; Clinton et al., 2010; Peterson, 2005; Singh and Glenn, 2009). These approaches have been largely successful at capturing broad-scale spatial patterns, but comparison with fine-scale field data often shows large errors at the local scale. This is further complicated by the fact that since the earliest remote sensing efforts to map cheatgrass invasion, additional species invasions have continued, and a larger suite of invasive species now dominate many plant communities of the Intermountain West region. For example, both medusahead (*Taeniatherum caput-medusae*) and wiregrass (*Ventenata dubia*) are Eurasian annual grasses that have dramatically expanded their ranges (Davies et al., 2013; Davies and Johnson, 2008; Tortorelli et al., 2020). Other invasive forbs, such as tansy mustard (*Descurainia pinnata* ssp. *intermedia*) and Russian thistle (*Kali tragus*) frequently co-occur and may have phenological patterns that are similar to or offset the phenological patterns of invasive grasses such as cheatgrass. Thus, commonly applied approaches that use satellite imagery to distinguish invasive annual grasses from native perennial vegetation according to their phenological differences tend to lump together multiple species sharing broadly similar phenological characteristics (e.g. “winter annual”), and do not achieve a species-specific classification of invasive plants.

Unoccupied aerial vehicles extend to larger areas the ability of field sampling to characterize the patchy distribution of plant communities, or even populations of a single species, at fine (<0.1 m) spatial resolution (Rominger and Meyer, 2019; Tay et al., 2018). A further advantage of UAVs is the ability to collect data repeatedly at user-determined intervals. By facilitating repeated sampling within a growing season, UAVs allow for a more highly resolved quantification of phenological variability in plant populations than could be accomplished with most satellite platforms.

Capitalizing on the ability of UAVs to carry out high-resolution, multi-temporal classification for mapping invasive plants to the species level, we develop a methodology for distinguishing two annual grass species that co-occur in the Intermountain West, cheatgrass and medusahead, from each other and from native vegetation. These two species are spectrally and structurally quite similar during their period of active growth but exhibit subtle yet significant differences in seasonal phenology (Fig. 1). Cheatgrass has a phenology typical of winter annual plant species, establishing from seed during the winter season, reaching its peak greenness early in the growing season, flowering and setting seed early (during which time it appears reddish), and then becoming senescent by late spring when most native perennial species of the Intermountain West are still green (Peterson, 2005). Medusahead stays green later in the season than cheatgrass and most other annual grasses and forbs (Dronova et al., 2017). Thus, our study area where the two invasive grass species co-occur provides an excellent test system for developing multi-temporal classification approaches to improve invasive plant mapping methodology. Both species are particularly problematic invasive weeds of the American West that are associated with losses of wildlife habitat and biodiversity, reduced forage production, and increased risk of wildfire (Knapp, 1996; Young, 1992). Both continue to expand their range through spread along roads and invasion of overgrazed rangelands, with increased propagule pressure leading to dominance of these species in near-monocultures following severe wildfire events (Balch et al., 2013). In our study area in western Nevada, USA we acquired frequent ($n = 8$ time periods) UAV imagery over the course of the growing season, to address the following questions:

1. Do phenological differences allow us to accurately distinguish the species, given the full time series of spectra available? How important is spectral variation over time, vs. spectral variation at a given point in time?
2. Which phenological stages (or sampling times) are most useful for distinguishing the species?
3. Which portions of the spectrum are most useful for distinguishing the species? Do we need near-infrared (NIR) spectral information, or does a phenologically informed analysis allow us to differentiate the species using only the visible bands?

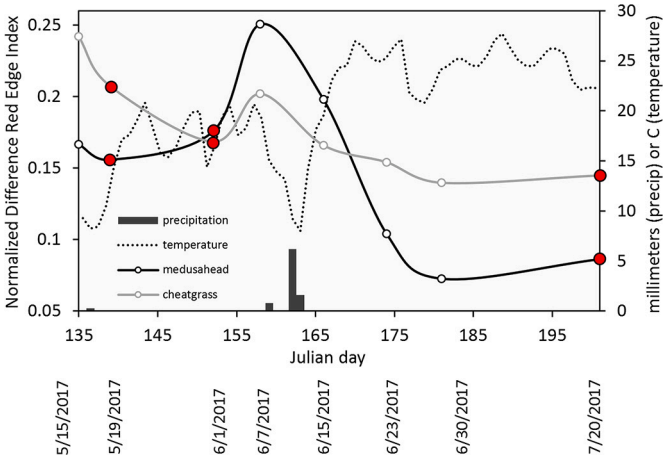

Fig. 1. Phenological curves showing Normalized Difference Red Edge Index (NDRE) for medusahead (solid black line) and cheatgrass (light gray line) along with the sampling dates (bubbles), for medusahead and cheatgrass plots MD-3 and CG-1. The x-axis shows the dates ordered from May 15 (Julian Day 135) with sampling dates for the flights depicted below. The three optimal sampling dates determined by this study are shown with the red bubbles. Precipitation (mm) and mean daily temperature (°C) are shown on the secondary y-axis. (For interpretation of the references to color in this figure legend, the reader is referred to the web version of this article.)

2. Materials and methods

2.1. Study area

The study area is located on the east flank of Peavine Mountain in Reno, Nevada at an elevation of 1646 m and a latitude 39.58° N (Fig. 2). The study site is located on a gentle slope (<5°) to the southwest spanning approximately 2.78 ha, having less than 7 m of relief. The area experiences a cold desert climate (i.e. hot, dry summers with cold, dry winters) with an annual average precipitation of 27.7 cm and the majority of precipitation falling as snow or rain during the winter months (Fig. 1). Average January minimum temperature is −5.8 °C, and average July maximum temperature is 31.5 °C (PRISM Group, 2015). Native vegetation consists of Wyoming big sagebrush (*Artemisia tridentata* ssp. *wyomingensis*), antelope bitterbrush (*Purshia tridentata*), broom snakeweed (*Gutierrezia sarothrae*), spineless horsebrush (*Tetradymia canescens*), and wide variety of native forbs, such as Anderson's clover (*Trifolium andersonii*), spreading groundsmoke (*Gayophytum diffusum*), fernleaf biscuitroot (*Lomatium dissectum*), jawleaf lupine (*Lupinus malacophyllus*), slender phlox (*Microsteris gracilis*), and spiny phlox (*Phlox hoodii*). There are also a wide variety of invasive species at this site included medusahead (*Taeniatherum caput-medusae*), cheatgrass (*Bromus tectorum*), Russian thistle (*Kali tragus*), redstem filaree (*Erodium cicutarium*), bur buttercup (*Ceratocephala testiculata*), prickly sow-thistle (*Sonchus asper*), and seeded crested wheatgrass (*Agropyron cristatum*). Site selection considerations were low relief, ease of access, and sufficient medusahead to obtain a representative sample, interspersed with common native species adjacent to sizable tracts (large patches >0.05 ha) of cheatgrass.

2.2. Data acquisition and processing

UAV imagery was collected across the growing seasons of medusahead and cheatgrass between the spring thaw and the summer dry down

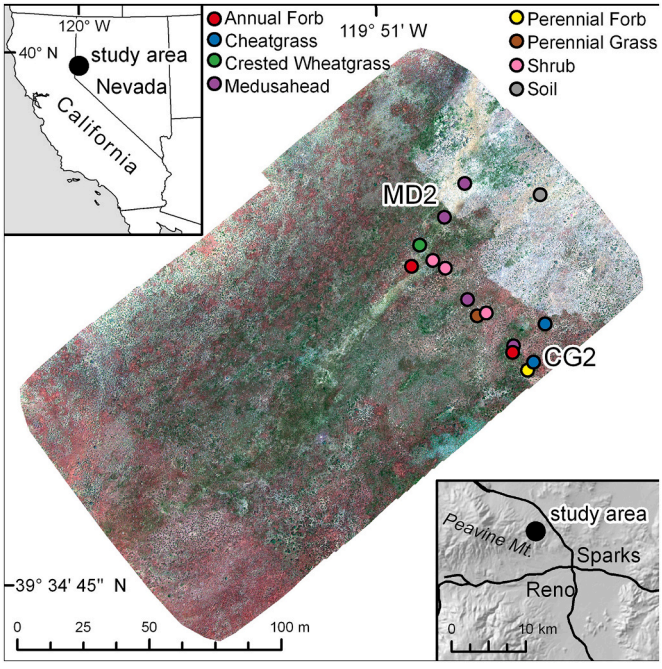

Fig. 2. UAV color-composite image taken on June 1, 2017 showing the location of the study area within Nevada relative to the location of the cities of Reno and Sparks and vegetation plots within the study area (yellow dots). MD2 and CG2 are the two representative medusahead and cheatgrass plots shown in Fig. 3. (For interpretation of the references to color in this figure legend, the reader is referred to the web version of this article.)

from May 15th to July 20th, 2017 (8 total flights – May 15, May 19, June 1, June 7, June 15, June 23, June 30, July 20). The 5-band spectral data were collected with a Micasense RedEdge sensor (https://support.micasense.com/hc/en-us/articles/360039671254) mounted on a Tarot quadcopter UAV platform flown at an altitude of approximately 30 m. Flight times were typically 45 min centered around solar noon and were based on pre-programmed flight plans using Universal Ground Control Software (UgCS) version 3.0.1302 software (SPH Engineering, Riga, Latvia) with a single battery swap and a single pass flight pattern. Photographs were captured ensuring 80% frontal overlap and 70% side overlap, as is needed to obtain an accurate digital surface model using photogrammetric software. The resulting data have 2-cm spatial resolution and spectral resolution of Blue (475 nm center, 20 nm bandwidth), Green (560 nm center, 20 nm bandwidth), Red (668 nm center, 10 nm bandwidth), Red Edge (717 nm center, 10 nm bandwidth), and NIR (840 nm center, 40 nm bandwidth). A MicaSense calibrated reflectance panel was used to calculate reflectance values from the RedEdge imagery; new calibration images were captured after each flight. Eight ground control point tiles were deployed for the duration of the study and used to co-align data from different flight dates and georeference the image stack using a Trimble R10 GPS receiver with RTX solutions (Trimble Inc., Sunnyvale, California, USA) with horizontal accuracy up to 8 mm and vertical accuracy up to 15 cm.

Composite rasters were processed in Pix4D v. 3.2 (Pix4D, Lausanne, Switzerland) using structure-from-motion (SfM) techniques that mosaicked images across all dates. Although Pix4D created a three-dimensional point cloud that is used to tie images together we did not use the height data in our classification of vegetation. All bands, across all time periods, were co-aligned in Pix4D resulting in an average horizontal positional precision of 1.26 cm. The eight ground-control points obtained from the Trimble were used to georeferenced the images into a NAD83 UTM Zone 11 projection. Calibration to reflectance was achieved with an empirical line approach (Smith and Milton, 1999) that took advantage of four spectrally diverse field targets that were laid out prior to each flight. Reference reflectance data were collected in the field on July 20, 2017 during cloud-free conditions just prior to the UAV flight using a Spectral Evolution SR-3500 (Spectral Evolution Inc., Haverhill, Massachussetts, USA). The SR-3500 collects data at 3-nm in the visible range. These data were resampled to match the band widths of the Micasense RedEdge camera and a linear regression was used to convert camera digital numbers to reflectance for each band individually.

Field vegetation data was collected using sixteen 1-m square quadrat frames on the day of each flight. Quadrat frames were located to ensure representative, homogeneous patches of the same vegetation types as used for classification. To ensure that quadrat frames were visible in each image we permanently placed four metal five-inch spikes at the corner of each frame, and we placed the frames on each of the metal spikes prior to each flight. Quadrat frame locations were initially collected with a Trimble GeoXT GPS unit (Trimble Inc., Sunnyvale, California, USA), and quadrats were re-photographed upon each subsequent visit. Initial vegetation measurements included estimating the aerial cover of each plant species as well as bare soil, rock, animal feces, medusahead litter, cheatgrass litter, and other plant litter. Each quadrat frame was classified (Fig. 2) into one of the following nine cover types based on its dominant vegetation type: annual forb, cheatgrass, crested wheatgrass, medusahead, litter, perennial forb, perennial grass, shrub, and bare soil. Slight differences in quadrat frame placement were accounted for such that pixels that had quadrat frames visible in them during any of the flights were removed. We randomly selected 9168 points from the resulting polygons to use for model training extracting each spectral band for each flight date. To obtain a fully independent validation we digitized polygons of dominant vegetation types and extracted 258,554 random points to use as validation. We manually digitized polygons using all eight dates of imagery as a background image coupled with extensive field knowledge of the site.

2.3. Image classification

We used the Random Forest algorithm to classify each pixel in the composite image into one of the nine dominant vegetation types. Random Forest is an ensemble decision tree classification in which trees are trained using bootstrapped sampling (Breiman, 2001). Random Forest has been extensively used for image classification because of its high performance, lack of reliance on an underlying data distribution, and its ability to handle both continuous and categorical predictors (Belgiu and Drăguţ, 2016; Pal, 2005). For this study we used the RandomForestSRC package in R (Ishwaran et al., 2008). Models were run in classification mode with default parameters using 1000 trees (ntree) and with the number of variables for splitting (mtry) set to the square root of the number of predictors. In order to compare the importance of different spectral wavelengths and different dates on the classification accuracy, we ran separate Random Forest models (i.e. virtual experiments) for All Bands (including NIR bands) vs. only RBG bands, across all possible combinations of one-date, two-date, and three-date image sets. Importance values for individual predictors (band*date combinations) were calculated using the mean decrease in impurity (Gini Index). Models were evaluated by creating a classification confusion matrix and assessing overall accuracy, Cohen's kappa, and by comparing the overall accuracy to that of a null model in which the probability of all classes is equal.

3. Results

3.1. Do phenological differences help to distinguish species?

The importance of species-specific phenology for distinguishing individual plant taxa was evidenced by the ability of multi-temporal models to provide superior classifications. This was particularly the case for the overall classification of 9 cover types for which there was a 10% decline in balanced classification accuracy, for the best single-date model compared to the best-fitting model that included all possible dates (54% vs. 64%). The best-fitting model had overall classification accuracy of 64.3% (95% CI: 64.1% - 64.5%) and a Cohen's Kappa of 0.55. We considered this to be a reasonably good classification accuracy given the relatively large number of plant cover types (9) that were classified and the expected level of spectral similarity among many of them (Table 1). Both cheatgrass and medusahead, the two target cover types of primary interest, were classified with high sensitivity (true positives; cheatgrass = 0.89, medusahead = 0.95) and high specificity (true negatives; cheatgrass = 0.90, medusahead = 0.90). Other plant cover types, however, were commonly misclassified. Annual forbs were classified with high specificity (0.99), but with a high proportion of false positives (0.85), likely due to the large number of spectrally distinct species included within this plant cover type. Other types with high specificity but a tendency towards false positives included crested wheatgrass (often misclassified when actually medusahead or litter) and shrubs (often misclassified when actually cheatgrass). Both cheatgrass and medusahead were commonly misclassified as perennial grass, which had a false positive proportion of 0.48 (Table 1). The perennial forb, litter, and soil types were classified with high accuracy, although litter and soil were often confounded with one another (Table 1). Visual inspection shows the skill of the classification in detecting and delineating patches of individual plant species (or even individual plants) at high resolution (~ 2 cm) (Fig. 3).

For overall classification accuracy (i.e. balanced accuracy across all nine cover types; Table 1), as well as for individual accuracy statistics for cheatgrass and medusahead classifications, the best models included at least three sampling dates (Table 2). Best models for individual species (cheatgrass or medusahead) were derived from just three dates (Table 3), whereas the best overall classification of all species required the maximum information available, all bands and all dates (Table 2). Three-date models were always superior to two-date and single-date models. Importantly, the most predictive three-date models differed across species with respect to which dates were sampled, reflecting differing phenologies of multiple plant species present (Fig. 1). Medusahead plants were still small and indistinct during the onset of active growth for cheatgrass; medusahead was still in its period of active growth when cheatgrass seed heads had matured ("red phase"); and cheatgrass had senesced by the time medusahead seed heads were produced.

3.2. What phenological stages, or sampling times, are most useful?

The best models for overall classification, as combinations of cameras and sampling dates, were not the optimal models for either medusahead or cheatgrass classification (Table 2). Furthermore, the best model for medusahead was not the best model for cheatgrass, and vice versa. However, there were three-date models that performed quite well for both species, with only small accuracy differences from their respective optimal models. For example, the model that best optimized classification accuracy across all taxa using just the visible bands (RGB 238) was the third best model overall (accuracy loss of 1.5%), the ninth best model for cheatgrass (accuracy loss of 1.9%), and the 55th best model for medusahead (accuracy loss of 4.2%). This model required three flights on May 19, June 1, and July 20, respectively. Images collected at these dates allowed differentiation of the two species according to their varying phenological development; note that cheatgrass transitioned from the green phase to an early senescent phase in the time

Table 1
Confusion matrix for the Random Forest classification model using all time periods and all spectral bands (i.e. full model) with field-mapped classes (reference data) in columns and model-predicted classes as rows. Values along the diagonal are correct predictions, values below the diagonal are false negatives, and values above the diagonal are false positives. The table includes accuracy statistics such as sensitivity (the proportion of true positives that are correctly identified), specificity (the proportion of true negatives who are correctly identified), and balanced accuracy ([sensitivity + specificity]/2).

Class	Reference data								
	Annual forb	Cheatgrass	Crested wheatgrass	Medusahead	Litter	Perennial forb	Perennial grass	Shrub	Soil
Annual Forb	9084	1068	25	117	4	578	124	86	18
Cheatgrass	10,453	19,729	82	427	0	345	1499	15,699	0
Crested Wheatgrass	26	54	2071	0	13	11	47	1372	1
Medusahead	14,629	660	958	101,231	48	325	1308	2584	27
Litter	19,327	0	1771	3256	8962	187	18	39	5615
Perennial Forb	6221	611	2	105	40	8359	107	4425	67
Perennial Grass	1957	81	166	1172	0	0	3635	328	0
Shrub	220	379	0	0	0	9	205	4944	0
Soil	243	2	23	0	4491	503	26	377	30,593
Total	62,160	22,584	5098	106,308	13,558	10,317	6969	29,854	36,321
Sensitivity	0.146	0.888	0.378	0.952	0.661	0.810	0.522	0.166	0.842
Specificity	0.991	0.895	0.995	0.890	0.892	0.959	0.987	0.997	0.978
Balanced Accuracy	0.569	0.892	0.686	0.921	0.776	0.885	0.754	0.581	0.910

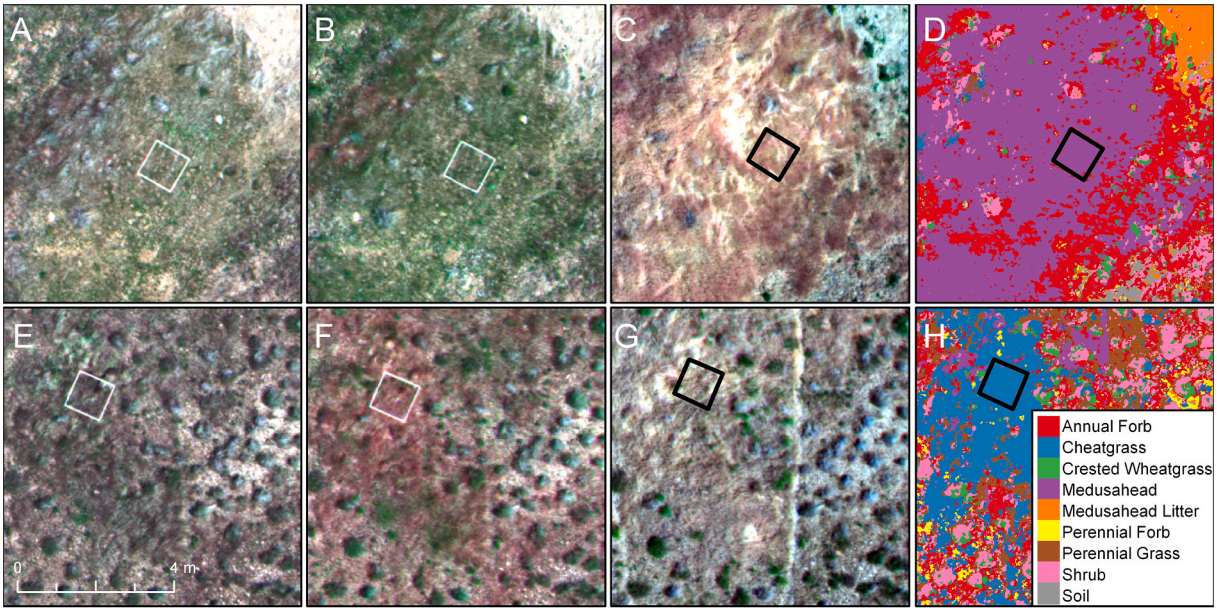

Fig. 3. Maps showing the three best imagery dates and vegetation classification for a representative medusahead and cheatgrass plot (labeled MD2 and CG2 in Fig. 2). Panels show A) medusahead quadrat May 19, B) medusahead quadrat June 1, C) medusahead quadrat July 20, D) classified map surrounding medusahead quadrat, E) cheatgrass quadrat May 19, F) cheatgrass quadrat June 1, G) cheatgrass quadrat July 20, H) classified map surrounding cheatgrass quadrat.

Table 2
Ten best overall ("all cover types") models ranked by classification accuracy and Cohen's kappa.

Experiment	Overall		Cheatgrass	Medusahead
	Accuracy	Kappa	Accuracy	Accuracy
All Bands, All Dates	0.645	0.557	0.861	0.921
RGB Only, All Dates	0.633	0.544	0.896	0.912
RGB Only, Days 2, 3, 8	0.630	0.535	0.901	0.887
RGB Only, Days 1, 3, 8	0.624	0.533	0.899	0.887
All Bands, Days 1, 5, 6	0.620	0.527	0.807	0.920
All Bands, Days 1, 5, 7	0.618	0.523	0.816	0.917
All Bands, Days 2, 3, 8	0.614	0.521	0.844	0.883
All Bands, Days 1, 3, 6	0.613	0.522	0.842	0.918
All Bands, Days 2, 3, 6	0.610	0.513	0.836	0.905
All Bands, Days 1, 6, 7	0.609	0.516	0.765	0.920

Table 3
Ten best models for medusahead and cheatgrass ranked by classification accuracy and Cohen's kappa.

	Experiment	Cheatgrass accuracy	Experiment	Medusahead accuracy
75	RGB Only, Days 1, 2, 3	0.920	All Bands, Days 5, 6, 7	0.929
81	RGB Only, Days 1, 3, 4	0.910	All Bands, All Dates	0.921
96	RGB Only, Days 2, 3, 4	0.909	All Bands, Days 1, 5, 6	0.920
99	RGB Only, Days 2, 3, 7	0.908	All Bands, Days 1, 6, 7	0.920
58	All Bands, Days 3, 4, 8	0.906	All Bands, Days 1, 3, 6	0.918
97	RGB Only, Days 2, 3, 5	0.904	All Bands, Days 1, 5, 7	0.917
57	All Bands, Days 3, 4, 7	0.904	All Bands, Days 3, 6, 7	0.916
13	RGB Only, Day 3	0.903	RGB Only, Days 5, 6, 7	0.915
100	RGB Only, Days 2, 3, 8	0.901	All Bands, Days 3, 5, 6	0.914
113	RGB Only, Days 3, 4, 7	0.901	All Bands, Days 3, 6, 8	0.913

period between May 19 and June 1 (Figs. 1, 3; Fig. S1). However, if the goal were to maximize prediction accuracy for medusahead while still providing accurate predictions for all taxa, an alternative model (ALL156) used data from all cameras including the NIR bands, was the fifth best model overall (accuracy loss of 2.5%), the 89th best model for cheatgrass (accuracy loss of 11.4%), and the third best model for medusahead (accuracy loss of 0.9%). For our field sites in 2017 this model required flights on May 15, June 15, and June 23.

Different dates proved more important depending upon whether the main objective of the study is to identify (a) cheatgrass, (b) medusahead, or (c) all major cover types. For example, variables from May 19, June 1, and June 7th had the highest variable importance factor for cheatgrass whereas June 7, June 23, and July 20th were most important for predicting medusahead (Fig. 4). In contrast, variable importance in predicting all cover classes was much more evenly spread across the eight dates.

3.3. What portions of the spectrum are most useful?

Although the information contributed by the NIR portion of the spectrum led to improved classification accuracy for medusahead and for mapping of all plant cover types (but not for cheatgrass individually), differences were small relative to classifications that used only the visible spectrum (Tables 3, 4). The RGB-only classifications also resulted in similar-looking maps with similar spatial distribution of classification error.

For classification of all plant cover types, the Red band consistently ranked high in variable importance score from the Random Forest analysis (Fig. 5a). The Blue band also ranked relatively high. The Green band generally ranked low except for the 3rd acquisition date, when cheatgrass was beginning to senesce and medusahead beginning to green up. The NIR (820–860 nm) and NIR Red Edge (712–722 nm) bands consistently ranked lower in importance.

The visible bands were also the most important for classifying cheatgrass, with the top five variables in importance alternating between Red and Green bands acquired on different dates (Fig. 5c). The two NIR bands (Red Edge and near-infrared) for May 19 and June 1, dates bounding the interval that separated the active growing stage of cheatgrass from its onset of senescence, also proved important. The

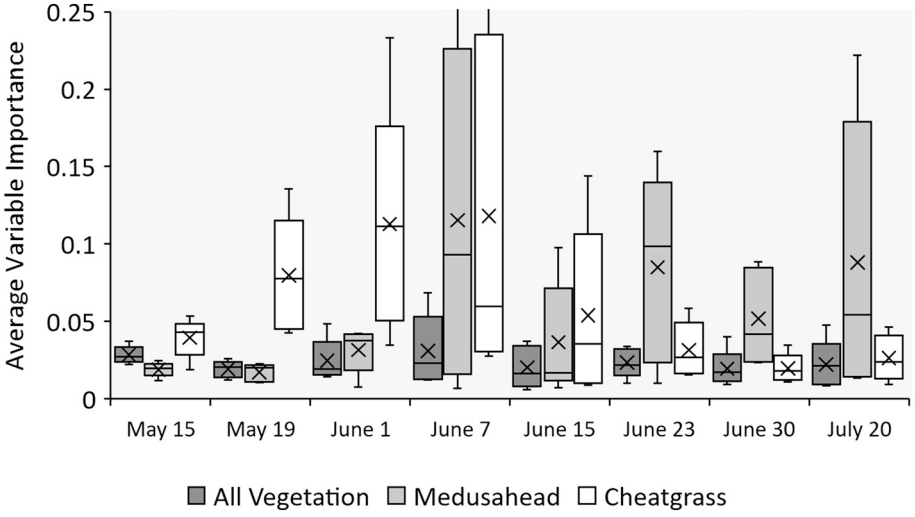

Fig. 4. Box and whisker plot showing the average variable importance by date pooling across spectral bands.

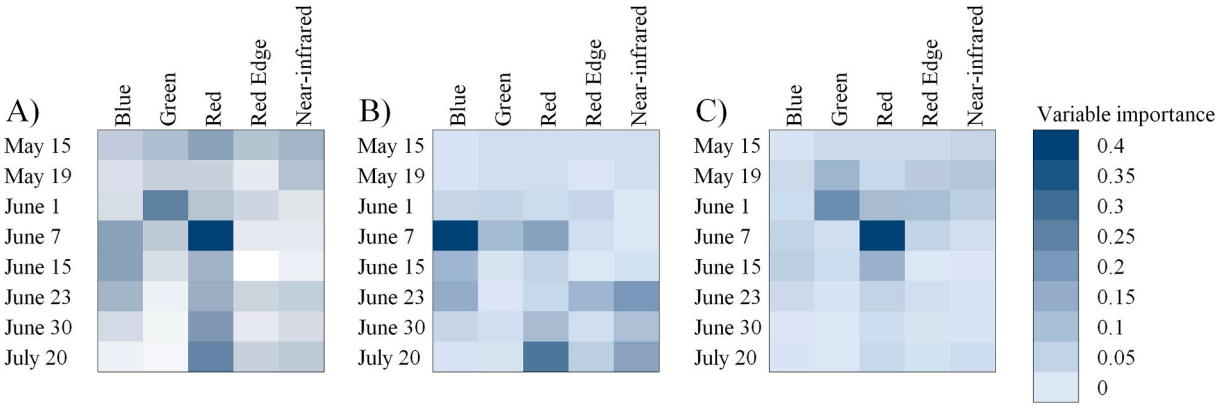

Fig. 5. Variable importance from the Random Forest models for A) all vegetation types classification, B) medusahead classification, and C) cheatgrass classification.

variable importance pattern was somewhat different for medusahead classification, where the Blue band on June 7 proved most important, and Blue, Red, and NIR bands acquired on different dates all proved important (Fig. 5b).

Average importance scores by band and by camera support the conclusion that the NIR camera and bands are less important than true-

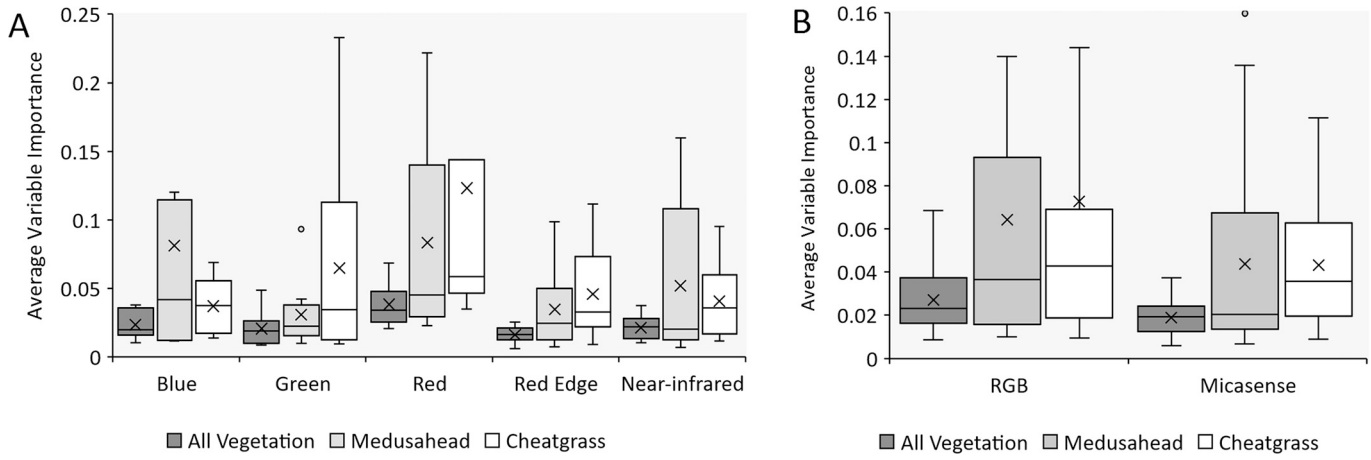

Fig. 6. Box and whisker plot showing the average variable importance values for spectral bands and cameras, pooling across flight dates. A) Average variable importance for all spectral bands for the "all vegetation" model, medusahead model, and cheatgrass model. B) Average variable importance for all spectral bands for the "all vegetation" model, medusahead model, and cheatgrass model. RGB bands include the Blue, Green, and Red wavelengths whereas the Micasense includes the additional Red Edge and NIR bands. (For interpretation of the references to color in this figure legend, the reader is referred to the web version of this article.)

color RGB cameras for detecting and classifying the plant cover types when multi-temporal imagery is available (Fig. 6). In particular, the Red band is vitally important for predicting annual grasses, such as cheatgrass and medusahead, and was consistently the most important variable (Fig. 5, Fig. 6a). Our results also suggest that the Blue band may outperform the Green band, particularly when it comes to predicting medusahead (Fig. 5, Fig. 6a). Finally, the utility of the Red Edge and NIR bands, while appearing to provide some unique information, may be largely diminished through the use of carefully timed flights that collect information at optimal phenological stages. When variable importance is averaged among the five variables of the Micasense camera, average variable importance is less than for the RGB cameras (Fig. 6b).

4. Discussion

Although our application remains limited in spatial extent, we have demonstrated multi-temporal classification as a viable tool to distinguish plants to the species level using often subtle phenological differences. More generalized remote sensing approaches, developed for mapping at regional scales, produce aggregated classification of multiple invasive species having roughly similar phenology. For example, invasive annual grasses of the western United States have been classified using differences in both intra-annual phenology (earlier green-up and senescence than native perennial vegetation) and inter-annual phenology (greater variability from year to year associated with annual precipitation). Peterson (2005) and Boyte et al. (2019) developed satellite-based classifications of annual grass cover that are based upon differences between spring NDVI and summer NDVI. The resulting classifications have been widely used to describe the relative dominance of invasive cheatgrass (*Bromus tectorum*) throughout the Intermountain West (e.g. Boyte et al., 2015; Boyte et al., 2016; Peterson, 2005). However, they are often not species-specific to cheatgrass and likely include diverse mixtures of various other native and non-native species with early-season phenology including medusahead, early-season mustards such as *Descurainia* spp., and early-season bunchgrasses such as Sandberg bluegrass (*Poa secunda*) and bottlebrush squirreltail (*Elymus elymoides*). Taking a different approach, other researchers have used the difference in vegetation index (VI) values between high and low rainfall years to classify invasive annual grasses according to their interannual variability relative to native perennial vegetation (Bradley and Mustard, 2005; Bradley and Mustard, 2006). Although the resulting classifications are sometimes interpreted to quantify abundance patterns of a single species (e.g. cheatgrass), other annual plant species can be confounded with the focal species of interest. Even when applied to an ecosystem where the focal species is the only dominant early-season annual grass species, the approach is insensitive to subsequent invasion by other invasive annual plants as is occurring throughout the Intermountain West region, where medusahead has been gradually replacing cheatgrass over the past half-century (Bateman et al., 2020; Hironaka, 1961; Hironaka, 1994; Torell et al., 1961), and where other invasive annual species such as wiregrass (*Ventanata dubia*) have steadily increased in dominance (Nicolli et al., 2020).

Our study further demonstrates that temporal information provides a substitute for more extensive spectral information obtained from a single point in time, as previously observed by others who have used multi-temporal classification to monitor vegetation phenology and dynamics (e.g. Sousa et al., 2019; Sousa and Davis, 2020). Previous efforts have accurately classified medusahead distribution and abundance from single-date imagery using NIR spectral information from airborne sensors, collected from either a single late-season image (Bateman et al., 2020), or from a single early-season image (Dronova et al., 2017). Similarly, the most accurate single-image classification from our study utilized information from NIR bands. However, a multi-temporal classification using imagery from three dates over the growing season did not require NIR information to achieve an optimal classification (Tables 3, 4). Indeed, the substitution of temporal for spectral information is well suited to UAV remote sensing, where the timing of image collection can be flexible. This substitution also can reduce the cost of invasive plant mapping in situations where more expensive multispectral or hyperspectral sensors are prohibitively expensive. However, UAV remote sensing can be inherently expensive due to the labor and computer hardware costs of the intensive image processing that is often required.

A remaining challenge to be resolved is the spatial variability in phenology (i.e. complex "phenological landscapes" sensu Cole and Sheldon, 2017), both within and between single species, that is present at both local and landscape scales. Cole and Sheldon (2017) found intraspecific variability in budburst timing of European trees to be related to elevation, spring temperature, habitat type, and soil type, with different environmental influences proving important for different tree species. At a given point in time, even a single species can exhibit substantial spatial variability in phenology associated with the physical environment (Andrew and Ustin, 2009; de Keyzer et al., 2017; Zhu et al., 2018). Trait variations among sub-populations or individuals within a single species can give rise to spatial variability in phenology, both at range-wide scales along regional climate gradients (e.g. *Fraxinus americana* throughout its North American range; Liang, 2019) and at finer spatial scales where genetic variability is high, or where clonal species occur in distinct patches (e.g. *Populus tremuloides*; Donaldson and Lindroth, 2008). Differences in disturbance history (Paritsis et al., 2006), herbivory and grazing management (Zhou et al., 2017), and the influence of historical land-use legacies also exert strong influences on spatial variability in plant phenology, although more research is needed. Particularly for herbaceous plants in arid and semi-arid landscapes, such spatial variability in phenology can occur over short distances (10s to 100 s of meters), is associated with fine-scale spectral variability even within a single species, and can be problematic for any phenologically-based approach to species-level vegetation classification.

Even where phenology is relatively uniform across a large area, phenological timing will vary from one growing season to the next due to interannual variability in temperature, precipitation, or other climate variables. This is particularly true for arid and semi-arid landscapes, where increasing aridity is generally associated with increasing interannual variability in precipitation, leading to pronounced resource pulses that strongly influence ecological dynamics (Chesson et al., 2004).

Because of such spatial and temporal variability in phenology both within and among plant species, the researcher will typically lack advance knowledge of the ideal timing for data acquisition for a given study landscape and year. Ultimately data acquisition in support of phenologically-based vegetation classification will be facilitated by improved methods for modeling phenological variation spatially across heterogeneous landscapes (Andrew and Ustin, 2009). Recent applications using land-based phenocams can provide suitable high-resolution data for developing models of phenological variation over fine spatial scales (Richardson et al., 2009; Snyder et al., 2019). In particular, the North American PhenoCam network holds great promise for providing long-term phenological information across environmentally diverse locations (Richardson et al., 2018).

The combination of high spatial and temporal variability in phenology for rangeland ecosystems presents a challenging problem for matching the timing of image acquisition with phenology. In addition to improved methods for modeling phenology over space and time, research teams seeking to implement a phenology-based multi-temporal classification approach will benefit from flexibility and the ability to mobilize rapidly to conduct data collection, as well as from local knowledge of site conditions and phenological status of plant species of interest.

We have demonstrated that it is possible, at the scale of an individual, well-characterized field site, to reliably distinguish multiple species of invasive annual grasses from each other and from co-occurring native species, using differences in plant phenology. The datasets arising from

such methodologies provide high-resolution information for modeling spatial patterns of invasive plant spread, or for quantifying the ecological risk of plant invasion at fine spatial scales. Practical implications of high-resolution, single-species mapping include improved early detection of novel plant invasions when patch sizes are still small and easy to control (i.e. "early detection rapid response" or EDRR). Control of invasive plants is most effective at the earliest stages of the invasion process (Pyšek and Richardson, 2010; Westbrooks, 2004), requiring mapping methods that can reliably detect invasives before they have already become dominant over extensive areas (Bradley, 2014; Hestir et al., 2008). High-resolution mapping at the species level can also support management of pathways and vectors for invasive plant establishment (e.g. Davies and Sheley, 2007). Additionally, although invasive plants were the focus of our particular study, species-level vegetation mapping should also prove valuable for monitoring and management of native plants of conservation concern.

Our UAV-based classification is limited in that only a relatively small area can realistically be mapped given current technological limitations. The feasibility of up-scaling our approach – while not clearly demonstrated in the current study – is suggested by other studies that have used high-resolution classifications of plant invasion as training data for broader-scale classifications of imagery from moderate-resolution satellite platforms such as Sentinel and Landsat (e.g. Bateman et al., 2020; Granzig et al., 2021). Bateman et al. (2020) used field data and 1-m aerial orthoimagery to train a classification of medusahead from a single late-summer Landsat scene across an extent of >370 km^2 (eastern Washington, USA), capitalizing on the unique spectral response of senesced medusahead relative to native plant species. For the >8000 km^2 Chiloé Island (south-central Chile), Granzig et al. (2021) used UAV orthoimages to train a Sentinel-2 time series for mapping an invasive shrub species (*Ulex europaeus*) with unique flowering phenology. Multiple studies have harmonized Landsat 8 and Sentinel-2 imagery to characterize land surface phenology over regional or continental extents (e.g., Bolton et al., 2020), including for the purpose of monitoring the spread and distribution of invasive annual grasses (Pastick et al., 2020). Although the spatial and temporal variability in phenology can greatly confound its utility for classifying aerial or satellite imagery to the species level, the use of remote sensing tools to quantify this variability is critical for advancing the science of phenological research, and for informing global models that simulate the interaction between climate and vegetation phenology (Morisette et al., 2009).

Credit author statement

PJW, JAG, TED, and SWT developed the concept and study design; CK, CS, HP, and TED planned and implemented data collection; KNJ, HP, and CK conducted image processing; KNJ, TED, and JAG analyzed and interpreted data; TED and AR prepared figures and tables; PJW led manuscript writing with primary contributions from TED and JAG and significant contributions from all authors.

Data availability statement

All data and imagery associated with this paper are available through the Dryad Digital Repository: doi:https://doi.org/10.5061/dryad.3ffbg79j2

Declaration of Competing Interest

The authors declare that they have no known competing financial interests or personal relationships that could have appeared to influence the work reported in this paper.

Acknowledgements

This research was funded by the Nevada Department of Wildlife (Habitat Conservation Fee Special Reserve Account) in a cooperative agreement with the USDA Forest Service Humboldt-Toiyabe National Forest (federal award 17-GN-11041730-25) to PJW, and by the National Science Foundation EAR award 1440506 to SWT. Contents of this paper are solely the responsibility of the authors and do not necessarily represent the official views of the Nevada Department of Wildlife or the United States Forest Service. UAV data collection and image processing were supported by the Centers for Transformative Environmental Monitoring Programs (CTEMPs) under National Science Foundation Awards EAR 1440506. The authors would like to thank Bobby Smith (Nevada Department of Wildlife; NDOW) and Monique Nelson (Humboldt-Toiyabe National Forest; HTNF) for providing critical programmatic and logistical support, as well as other project collaborators from HTNF including Meagan Carter, Boyd Hatch, and Dirk Netz. In addition, the authors thank Dan Sousa, one anonymous reviewer, and Associate Editor Geoffrey Henebry for their helpful comments.

Appendix A. Supplementary data

Supplementary data to this article can be found online at https://doi.org/10.1016/j.rse.2021.112568.

References

Andrew, M.E., Ustin, S.L., 2009. Effects of microtopography and hydrology on phenology of an invasive herb. Ecography 32, 860–870.
Balch, J.K., Bradley, B.A., D'Antonio, C.M., Gómez-Dans, J., 2013. Introduced annual grass increases regional fire activity across the arid western USA (1980–2009). Glob. Chang. Biol. 19, 173–183.
Bateman, T.M., Villalba, J.J., Ramsey, R.D., Sant, E.D., 2020. A multi-scale approach to predict the fractional cover of medusahead (*Taeniatherum caput-medusae*). Rangel. Ecol. Manag. 73, 538–546.
Belgiu, M., Drăguț, L., 2016. Random forest in remote sensing: a review of applications and future directions. ISPRS J. Photogramm. Remote Sens. 114, 24–31.
Bolton, D.K., Gray, J.M., Melaas, E.K., Moon, M., Eklundh, L., Friedl, M.A., 2020. Continental-scale land surface phenology from harmonized Landsat 8 and Sentinel-2 imagery. Remote Sens. Environ. 240, 111685.
Boyte, S.P., Wylie, B.K., Major, D.J., 2015. Mapping and monitoring cheatgrass dieoff in rangelands of the Northern Great Basin, USA. Rangel. Ecol. Manag. 69, 18–28.
Boyte, S.P., Wylie, B.K., Major, D.J., 2016. Cheatgrass percent cover change: comparing recent estimates to climate change– driven predictions in the Northern Great Basin. Rangel. Ecol. Manag. 69, 265–279.
Boyte, S.P., Wylie, B.K., Major, D.J., 2019. Validating a time series of annual grass percent cover in the sagebrush ecosystem. Rangel. Ecol. Manag. 72, 347–359.
Bradley, B.A., 2014. Remote detection of invasive plants: a review of spectral, textural and phenological approaches. Biol. Invasions 16, 1411–1425.
Bradley, B.A., Mustard, J.F., 2005. Identifying land cover variability distinct from land cover change: cheatgrass in the Great Basin. Remote Sens. Environ. 94, 204–213.
Bradley, B.A., Mustard, J.F., 2006. Characterizing the landscape dynamics of an invasive plant and risk of invasion using remote sensing. Ecol. Appl. 16, 1132–1147.
Breiman, L., 2001. Random forests. Mach. Learn. 45, 5–32.
Chesson, P., Gebauer, R.L., Schwinning, S., Huntly, N., Wiegand, K., Ernest, M.S., Sher, A., Novoplansky, A., Weltzin, J.F., 2004. Resource pulses, species interactions, and diversity maintenance in arid and semi-arid environments. Oecologia 141, 236–253.
Clinton, N.E., Potter, C., Crabtree, B., Genovese, V., Gross, P., Gong, P., 2010. Remote sensing–based time-series analysis of cheatgrass (*Bromus tectorum L.*) phenology. J. Environ. Qual. 39, 955–963.
Cole, E.F., Sheldon, B.C., 2017. The shifting phenological landscape: within-and between-species variation in leaf emergence in a mixed-deciduous woodland. Ecol. Evolut. 7, 1135–1147.
Davies, K.W., Johnson, D.D., 2008. Managing medusahead in the Intermountain West is at a critical threshold. Rangelands 30, 13–15.
Davies, K.W., Sheley, R.L., 2007. A conceptual framework for preventing the spatial dispersal of invasive plants. Weed Sci. 55, 178–184.
Davies, K.W., Nafus, A.M., Madsen, M.D., 2013. Medusahead invasion along unimproved roads, animal trails, and random transects. Western North Am. Nat. 73, 54–59.
de Keyzer, C.W., Rafferty, N.E., Inouye, D.W., Thomson, J.D., 2017. Confounding effects of spatial variation on shifts in phenology. Glob. Chang. Biol. 23, 1783–1791.
Donaldson, J.R., Lindroth, R.L., 2008. Effects of variable phytochemistry and budbreak phenology on defoliation of aspen during a forest tent caterpillar outbreak. Agric. For. Entomol. 10, 399–410.
Dronova, I., Spotsweed, E.N., Suding, K.N., 2017. Opportunities and constraints in characterizing landscape distribution of an invasive grass from very high resolution multi-spectral imagery. Front. Plant Sci. 8, 890.
Granzig, T., Fassnacht, F.E., Kleinschmit, B., Forster, M., 2021. Int. J. Appl. Earth Obs. Geoinf. 96, 102281.
Hestir, E.L., Khanna, S., Andrew, M.E., Santos, M.J., Viers, J.H., Greenberg, J.A., Rajapakse, S.S., Ustin, S.L., 2008. Identification of invasive vegetation using

hyperspectral remote sensing in the California Delta ecosystem. Remote Sens. Environ. 112, 4034–4047.
Hironaka, M., 1961. The relative rate of root development of cheatgrass and medusahead. J. Range Manag. 14, 263–267.
Hironaka, M., 1994. Medusahead: natural successor to the cheatgrass type in the Northern Great Basin. In: Monsen, S.B., Kitchen, S.G. (Eds.), Proceedings: Ecology and Management of Annual Rangelands. USDA Forest Service General Technical Report INT-GTR-313, pp. 85–102.
Ishwaran, H., Kogalur, U.B., Blackstone, E.H., Lauer, M.S., 2008. Random survival forests. Ann. Appl. Stat. 2, 841–860.
Knapp, P.A., 1996. Cheatgrass (*Bromus tectorum*) dominance in the Great Basin desert: history, persistence, and influences to human activities. Glob. Environ. Chang. 6, 37–52.
Liang, L., 2019. A spatially explicit modeling analysis of adaptive variation in temperate tree phenology. Agric. For. Meteorol. 266, 73–86.
Martin, F.M., Müllerová, J., Borgniet, L., Dommanget, F., Breton, V., Evette, A., 2018. Using single-and multi-date UAV and satellite imagery to accurately monitor invasive knotweed species. Remote Sens. 10, 1662.
Marushia, R.G., Cadotte, M.W., Holt, J.S., 2010. Phenology as a basis for management of exotic annual plants in desert invasions. J. Appl. Ecol. 47, 1290–1299.
Morisette, J.T., Richardson, A.D., Knapp, A.K., Fisher, J.I., Graham, E.A., Abatzoglou, J., Wilson, B.E., Breshears, D.D., Henebry, G.M., Hanes, J.M., Liang, L., 2009. Tracking the rhythm of the seasons in the face of global change; phenological research in the 21st century. Front. Ecol. Environ. 7, 253–260.
Müllerová, J., Brůna, J., Bartaloš, T., Dvořák, P., Vitkova, M., Pyšek, P., 2017. Timing is important: Unmanned aircraft vs. satellite imagery in plant invasion monitoring. Front. Plant Sci. 8, 887.
Nicolli, M., Rodhouse, T.J., Stucki, D.S., Shinderman, M., 2020. Rapid invasion by the annual grass *Ventenata dubia* into protected-area, low-elevation sagebrush steppe. Western North Am. Nat. 80, 243–252.
Ogden, J.A.E., Rejmánek, M., 2005. Recovery of native plant communities after the control of a dominant invasive plant species, *Foeniculum vulgare*: implications for management. Biol. Conserv. 125, 427–439.
Pal, M., 2005. Random forest classifier for remote sensing classification. Int. J. Remote Sens. 26, 217–222.
Paritsis, J., Raffaele, E., Veblen, T.T., 2006. Vegetation disturbance by fire affects plant reproductive phenology in a shrubland community in northwestern Patagonia, Argentina. N. Z. J. Ecol. 30, 387–395.
Pastick, N.J., Dahal, D., Wylie, B.K., Parajuli, S., Boyte, S.P., Wu, Z.T., 2020. Characterizing land surface phenology and exotic annual grasses in dryland ecosystems using Landsat and Sentinel-2 data in harmony. Remote Sens. 12, 725.
Peterson, E.B., 2005. Estimating cover of an invasive grass (*Bromus tectorum*) using tobit regression and phenology derived from two dates of Landsat ETM+ data. Int. J. Remote Sens. 26, 2491–2507.
Pimentel, D., McNair, S., Janecka, J., Wightman, J., Simmonds, C., O'Connell, C., Wong, E., Russel, L., Zern, J., Aquino, T., Tsomondo, T., 2001. Economic and environmental threats of alien plant, animal, and microbe invasions. Agric. Ecosyst. Environ. 84, 1–20.
PRISM Group, 2015. PRISM climatological normals, 1981–2010. The PRISM Group, Oregon State University, Corvallis, OR.
Pyšek, P., Richardson, D.M., 2010. Invasive species, environmental change and management, and health. Annu. Rev. Environ. Resour. 35, 25–55.
Richardson, A.D., Braswell, B.H., Hollinger, D.Y., Jenkins, J.P., Ollinger, S.V., 2009. Near-surface remote sensing of spatial and temporal variation in canopy phenology. Ecol. Appl. 19, 1417–1428.
Richardson, A.D., Hufkens, K., Milliman, T., Aubrecht, D.M., Chen, M., Gray, J.M., Johnston, M.R., Keenan, T.F., Klosterman, S.T., Kosmala, M., Melaas, E.K., Friedl, M. A., Frolking, S., 2018. Tracking vegetation phenology across diverse North American biomes using PhenoCam imagery. Sci. Data 5, 180028.
Rominger, K., Meyer, S.E., 2019. Application of UAV-based methodology for census of an endangered plant species in a fragile habitat. Remote Sens. 11, 719.
Singh, N., Glenn, N.F., 2009. Multitemporal spectral analysis for cheatgrass (*Bromus tectorum*) classification. Int. J. Remote Sens. 30, 3441–3462.
Smith, G.M., Milton, E.J., 1999. The use of the empirical line method to calibrate remotely sensed data to reflectance. Int. J. Remote Sens. 20, 2653–2662.
Snyder, K.A., Huntington, J.L., Wehan, B.L., Morton, C.G., Stringham, T.K., 2019. Comparison of Landsat and land-based phenology camera normalized difference vegetation index (NDVI) for dominant plant communities in the great basin. Sensors 19, 1139.
Sousa, D., Davis, F.W., 2020. Scalable mapping and monitoring of Meditarranean-climate oak landscapes with temporal mixture models. Remote Sens. Environ. 247, 111937.
Sousa, D., Small, C., Spalton, A., Kwarteng, A., 2019. Coupled spatiotemporal characterization of monsoon cloud cover and vegetation phenology. Remote Sens. 11 (10), 1203.
Tay, J.Y., Erfmeier, A., Kalwij, J.M., 2018. Reaching new heights: can drones replace current methods to study plant population dynamics? Plant Ecol. 219, 1139–1150.
Torell, P.J., Erickson, L.C., Haas, R.H., 1961. The medusahead problem in Idaho. Weeds 9, 124–131.
Tortorelli, C.M., Krawchuk, M.A., Kerns, B.K., 2020. Expanding the invasion footprint: *Ventenata dubia* and relationships to wildfire, environment, and plant communities in the Blue Mountains of the Inland Northwest, USA. Appl. Veg. Sci. 49, 683–696.
Westbrooks, R.G., 2004. New approaches for early detection and rapid response to invasive plants in the United States. Weed Technol. 18, 1468–1472.
Wilcove, D.S., Rothstein, D., Dubow, J., Phillips, A., Losos, E., 1998. Quantifying threats to imperiled species in the United States. BioScience 48, 607–615.
Young, J.A., 1992. Ecology and management of medusahead (*Taeniatherum caput-medusae* ssp. *asperum* Melderis). Great Basin Nat. 52, 245–252.
Zhou, Y., Xiao, X., Wagle, P., Bajgain, R., Mahan, H., Basara, J.B., Dong, J., Qin, Y., Zhang, G., Luo, Y., Gowda, P.H., 2017. Examining the short-term impacts of diverse management practices on plant phenology and carbon fluxes of Old World bluestems pasture. Agric. For. Meteorol. 237, 60–70.
Zhu, W., Zheng, Z., Jiang, N., Zhang, D., 2018. A comparative analysis of the spatio-temporal variation in the phenologies of two herbaceous species and associated climatic driving factors on the Tibetan Plateau. Agric. For. Meteorol. 248, 177–184.